SIMULATION OF COMPLEX 3D NON-PLANAR CRACK PROPAGATION USING ROBUST ADAPTIVE RE-MESHING AND RADIAL BASIS FUNCTIONS

C. Timbrell, A. Maligno (Zentech International Limited, UK);
D.Stevens (BLOS International, UK).

Presenter: C. Timbrell, Principal Engineer

THEME

Structural Analysis - Durability, Fatigue & Fracture

SUMMARY

An improved numerical technique for complex shaped non-planar three-dimensional crack growth simulations is proposed. This technique couples the adaptive re-meshing method used during crack growth simulation in the FE-based fracture mechanics code Zencrack with mesh relaxation using radial basis functions. This allows the uninterrupted simulation of crack propagation in engineering structures where the component geometries and local loading conditions may develop complex 3D crack configurations.

Collocation with radial basis functions (RBFs) is an effective methodology for the interpolation of arbitrary scalar and vector fields defined over scattered datasets. By defining a mesh displacement field over a volumetric domain, the RBF collocation approach may be used to smoothly map a user-defined displacement of elements onto the entire domain, thereby “relaxing” the mesh around the imposed displacements. This mesh deformation leads, in most cases, to significantly improved element quality in comparison to traditional mesh-relaxation approaches such as Laplacian relaxation. In particular, elements that lie close to the source of a large displacement can be expected to exhibit significantly improved characteristics (such as aspect ratio and skew) in comparison to traditional approaches.

The application of RBF deformation to fracture-tracking problems introduces many additional complexities that require novel and creative solutions. The most significant of these is the large difference in length scales between the imposed deformations - which are of element scale, and the constraints at the domain boundaries - which are of problem-scale. These differences in length scales make the problem unsuitable for use with compactly supported collocation methods. To retain a computationally efficient interpolation which is scalable to large problem sizes, a new method for RBF collocation has been

developed which is based on large numbers of overlapping local collocation systems, using the underlying elemental structure as a framework. By linking together these overlapping local collocation systems a sparse global matrix may be formed, which can be solved to obtain the displacement at each node within the relaxation domain.

For crack propagation simulation it is desirable to allow the mesh to move freely within the domain, as defined by the imposed displacements around the crack-tip, and to constrain the motion of surface and edge nodes such that they remain within their pre-existing geometric surfaces. In this work we describe surface-constraint methods which are suitable for use with complex 3D geometries where the mesh relaxation is performed using globally or locally supported RBF collocation systems.

KEYWORDS

Finite element method, crack propagation, mesh relaxation, radial basis functions, finite collocation.

SIMULATION OF COMPLEX 3D NON-PLANAR CRACK PROPAGATION USING ROBUST ADAPTIVE RE-MESHING AND RADIAL BASIS FUNCTIONS

1: Introduction

The simulation of crack propagation using the Finite Element Method (FEM) introduces a number of significant numerical challenges, owing to the large concentration of stresses that are present on approach to the crack front; a line-singularity which advances though the solution domain based on the local stress intensity factor. The mesh must be refined significantly on approach to the crack front in order to capture the rapid change in stresses. Further, in order to model the propagation of the crack-front, updated meshes must be constructed as the crack advances in the domain. This means that careful treatment of the elements surrounding the crack region is required; the surrounding mesh must be "relaxed" around the crack region in order to retain element quality throughout the domain. The re-meshing process which needs to be undertaken can be considered as:

- Advance the nodes on the crack front to the required new positions in accordance with the fracture mechanics conditions along the crack, the material data and the load history.

- Calculate a set of movements (i.e. deformations or displacements) to apply to the remaining mesh nodes to generate a full set of updated node coordinates for the advanced crack position, ensuring that surface, edge and corner information is retained.

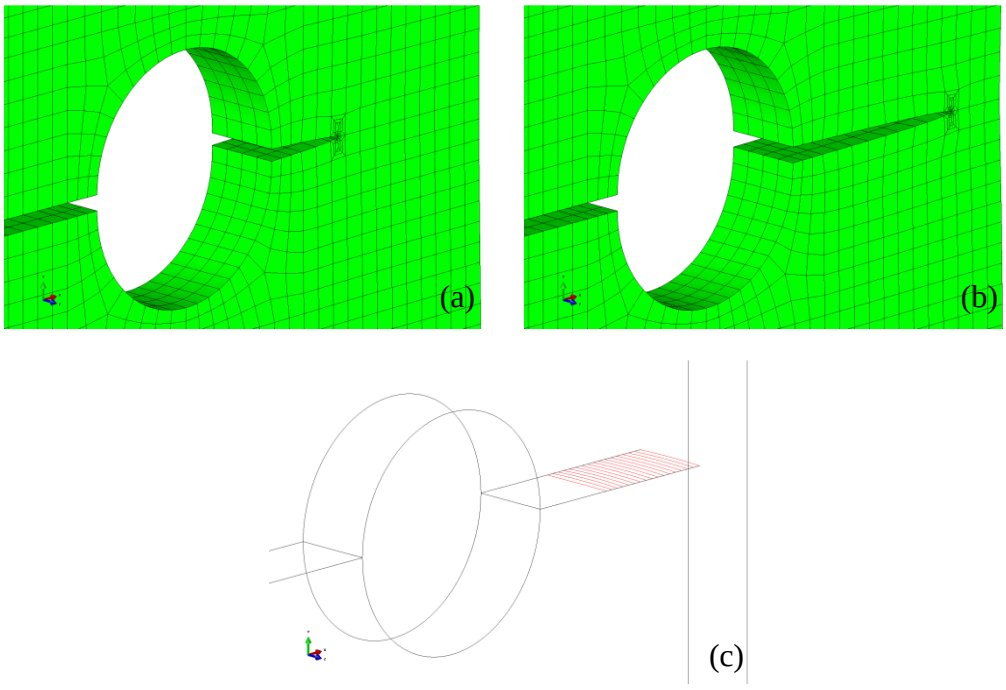

Figure 1: Example of typical meshes from planar crack growth at a hole feature. (a) initial crack mesh, (b) final crack mesh, (c) calculated crack front positions as the crack advances through the domain.

SIMULATION OF COMPLEX 3D NON-PLANAR CRACK PROPAGATION USING ROBUST ADAPTIVE RE-MESHING AND RADIAL BASIS FUNCTIONS

Traditional mesh relaxation techniques, such as local Laplacian relaxation technique (see for example Jones (1974)), rely on analysing the quality of individual elements and adjusting nodal positions in an attempt to retain well-formed elements. An alternative approach can be found in the form of radial basis function (RBF) collocation methods. Rather than moving nodes based on the properties of individual elements, RBF collocation methods allow for a smooth mapping of a deformation, which is defined at a subset of nodes, across the entire solution domain. In this way, the RBF collocation approach can be seen as somewhat independent from the underlying computational mesh; the deformation is computed as a smooth and continuous function defined over the entire solution domain, and the motion of nodes within the mesh is computed by reconstructing the value of this interpolation function at each nodal location.

The strength of the RBF collocation approach for such mesh deformation problems has been demonstrated by Bos (2010). In this work, RBF collocation is used to relax a computational mesh for the CFD simulation of flapping wing flight. In this case the periodic motion of the wings represents a source of deformation – analogous to the motion of the crack-front in the present work, and the RBF collocation approach is used to relax the surrounding computational mesh around this predefined wing motion. The performance of the RBF method was compared to a number of traditional, element-analysis based relaxation techniques, and is found to offer significantly improved mesh quality – particularly in the case of large deformations with rotating and twisting wing motion.

The simulation of crack propagation introduces additional challenges for mesh relaxation, primarily related to the presence of complex geometries and the necessity to appropriately constrain the motion of surface and edge nodes. Such nodes must be free to move in order to maintain element quality, but must be constrained to their respective surface or edge in order to retain the shape of the domain geometry. This presents an additional challenge for relaxation with RBF collocation methods, as the length scale of the deformation source (which is of element-scale) may be orders of magnitude smaller than the length scale of the domain. Such issues are not present in the simulation of insect-wing motion, as described by Bos, where the magnitude of mesh motion simply decays to zero in the open boundaries of the far-field.

2: Globally supported RBF collocation

The RBF collocation formulation was originally formulated by Hardy (1971), for the smooth interpolation of scattered pointwise datasets. The use of RBF methods for such purposes gained significant support following a review by Franke (1982), which compared all available methods for scattered data interpolation, concluding that RBF collocation offered the most accurate and stable results.

A radial basis function depends upon the separation distances of a set of functional centres, known as trial points, and exhibits spherical symmetry around these centres. There are several commonly used radial basis functions, however in this work we will focus on the popular multiquadric function, with $m=1$:

$$\psi(r)=\left(r^2+c^2\right)^{\frac{m}{2}} \tag{1}$$

The multiquadric RBF is a conditionally positive definite function of order m, which requires the addition of a polynomial term of order $(m-1)$, together with a homogeneous constraint condition, in order to obtain an invertible interpolation matrix. By choosing $m=1$, the polynomial term reduces to the addition of a constant. The c term is known as the shape parameter, and defines the relative flatness of the basis functions, with larger values of c representing flatter basis functions. In practice, the tuning of this parameter can effect the quality of the interpolation obtained. In general, higher values of c lead to the more accurate interpolation of smooth data, at the cost of greater numerical ill-conditioning in the resulting collocation matrices (see, for example, Kansa (1992), Fornberg and Zuev (2007)).

For a series of scattered data, u_j, located at N quasi-randomly trial locations ξ_j, the RBF approximation to the continuous solution field, $u(x)$, is given by:

$$u(x)=\sum_{j=1}^{N}\alpha_j\psi\left(\left\|x-\xi_j\right\|\right)+\sum\alpha_{j+N}P_{m-1}^{j}(x) \qquad x\in\Re^n \tag{2}$$

Where P_{m-1}^{j} is the j^{th} term of an order $(m-1)$ polynomial, under the constraint

$$\sum_{j=1}^{N}\alpha_j P_{m-1}^{k}\left(x_j\right)=0 \qquad k=1,...,NP \tag{3}$$

with NP being the total number of terms in the polynomial (equal to one for the $(m=1)$ case considered in this work).

By enforcing equation (2) at N distinct locations x_j, coinciding with the functional centres ξ_j, a symmetric and positive-definite collocation system can be formed to determine the functional weights α_j:

$$\begin{pmatrix}\psi_{ij} & P_{m-1}\\ P_{m-1} & 0\end{pmatrix}\alpha_i=\begin{pmatrix}u_i\\ 0\end{pmatrix} \tag{4}$$

The globally supported basis functions (1) lead to a fully populated linear system, with each functional centre influencing the solution construction at every x_j. While this approach allows for excellent convergence rates, it results in a computational cost of, at best, $O\left(N^2\right)$, making the approach computationally inefficient for application to large datasets. Moreover, as the size of the dataset increases, the numerical conditioning of the collocation matrix worsens, particularly in the case of flat basis functions, i.e. large values of the shape parameter c - see Schaback (1993) for more detail.

To mitigate the computational cost and numerical conditioning issues, Wendland (1995) and Wu (1995) developed a series of compactly supported radial basis functions. These CSRBF functions are non-zero only within a locally supported radius. In this way, the reconstruction of the solution field $u(x)$ is generated only from functional centres in the immediate vicinity of the reconstruction location x, resulting in a sparsely-populated linear system which can be scaled to arbitrarily-large datasets.

Compact support RBF methods are commonly used for a number of applications, most notably for the reconstruction of complex geometric surfaces, for example in computer graphics applications. However, they are not well suited to mesh relaxation in the case of crack propagation. In this case the source of the deformation; i.e. the advancement of the crack-front through the domain, can be expected to be separated from the surface nodes, at which constraint conditions are required, by a distance of the order of the problem scale. Therefore, in order to link the nodes at the crack-front to those at the geometric surface, the support radius must be of the same order as the size of the domain. In this way a fully-populated collocation matrix is produced, bringing with it the aforementioned issues of scalability and numerical conditioning.

3: Local RBF finite collocation approach

An alternative to compactly-supported RBF collocation methods can be found by dividing the solution domain into a series of small, highly overlapping RBF collocation systems. Over each sub-domain an RBF collocation is performed, thereby providing an expression for the value of the interpolation function in terms of its value at the surrounding nodes. By assembling these reconstructions in an appropriate manner, a sparse global system is formed that can be solved to obtain the value of the solution field at each internal node. In this way the method is scalable to large problem sizes; although the individual local collocation systems are themselves fully populated, they are sufficiently small that they can be solved efficiently. Such local RBF approaches retain much of the flexibility of global approaches, without suffering from the computational cost and numerical conditioning issues as the dataset size grows.

Local RBF collocation approaches offer the flexibility to not only perform interpolation, but also to solve arbitrary PDEs over the solution domain. Such approaches have been used to formulate meshless finite difference methods; see Wright and Fornberg (2007), Divo and Kassab (2007), Stevens et. al (2009). In this RBF-FD approach the radial basis functions replicate the role of polynomial interpolants in traditional finite difference methods, allowing the value of the PDE to be reconstructed at the local system centrepoint. By solving an appropriate PDE, rather than performing a simple interpolation, it is possible to further smooth the motion of nodes during the mesh relaxation process. Moreover, a well-posed PDE with appropriate boundary conditions has a unique solution, whereas a pure interpolation is potentially subject to unknown behaviour in the regions between collocation centres.

In this work we propose to solve the steady heat equation (5) over the entire solution domain, using a local RBF collocation method. In this way each of the three displacement components, as enforced at each of the crack-tip positions to describe the advancement of the crack through the mesh, act as a source of heat. This heat is then smoothly diffused among surrounding mesh nodes, as defined by the solution of the heat equation. Any other fixed nodes, such as those at geometric corners, act as fixed-temperature nodes; i.e. Dirichlet boundary conditions (6). At all remaining surface nodes an adiabatic condition is enforced (7).

$$\frac{\partial^2 u_i}{\partial x_k^2} = 0 \qquad i = 1,2,3 \tag{5}$$

$$u_i = f_i(x) \qquad i = 1,2,3 \tag{6}$$

$$n_j \frac{\partial u_i}{\partial x_j} = 0 \qquad i = 1,2,3 \tag{7}$$

While a meshless finite difference method may be suitable to solve the proposed formulation, we use instead the related “finite collocation” approach, as described by Stevens et. al (2012). In the finite collocation approach, as with the RBF-FD approach described above, local RBF collocation systems are formed around each internal node by connecting them to neighbouring mesh-nodes. However, in this case the RBF interpolants do themselves satisfy the governing PDE and boundary operators, and the global assembly is obtained by simply reconstructing the value of the interpolated function (i.e. the nodal displacement) at the local system centrepoint, rather than by reconstructing the value of the PDE as in RBF-FD. In Stevens et. al (2012) it is demonstrated that, for a wide range of convection-diffusion problems, the finite collocation approach offers superior convergence rates and, more importantly in the context of this work, better stability to variations in basis function flatness, in comparison to RBF-FD methods on equivalent stencils.

To form the set of neighbour nodes for a given internal focus-node, we first identify the set of elements which include the focus node, and add to the stencil all nodes that are contained by these elements. In this way, 27 mesh-nodes are included in each RBF collocation system. In addition, the centres of the set of elements are added, and at these locations the governing PDE, i.e. the heat equation, is enforced (see Figure 2). In the case that a stencil includes nodes located on the domain boundary, the appropriate boundary condition is enforced instead. Note that at the central node of the stencil the governing partial differential operator is enforced, in contrast to all other mesh-nodes, where the displacement value is enforced. This is to allow the displacement value to be reconstructed at this location later in the solution procedure, in order to form the sparse global assembly.

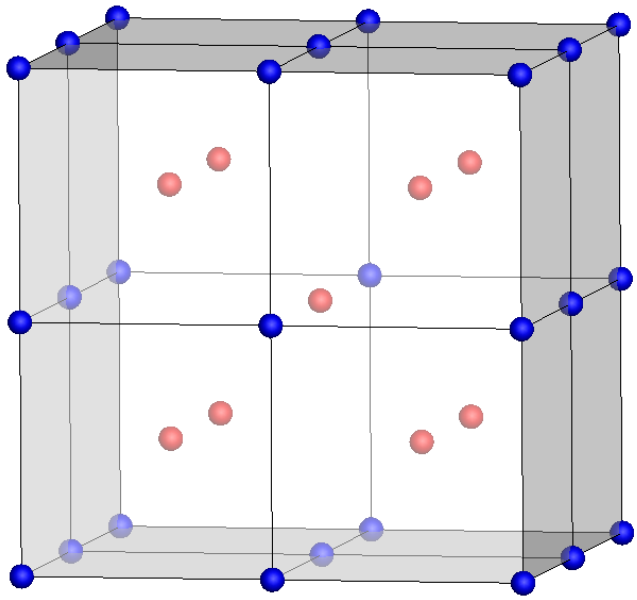

Figure 2: Schematic representation of stencils for finite collocation. Blue spheres represent solution centres, at which the displacement is collocated. Red spheres represent collocation of the governing partial differential operator.

The enforcement of arbitrary partial differential operators, specifically the governing PDE and adiabatic boundary conditions, is obtained by forming an Hermitian RBF collocation system. The Hermitian RBF collocation formulation was formulated by Fasshauer (1997), and extends the basic RBF formulation (2) by including the influence of the partial differential operators within the solution construction.

We define the governing partial differential operator, L, over the domain Ω as

$$L[u_i] = \frac{\partial^2}{\partial x_j^2}[u_i] = 0 \qquad i = 1,2,3 \tag{8}$$

and define the boundary operator, B, over the domain boundary Γ either as Dirichlet type

$$B[u_i] = u_i = f_i(x) \qquad i = 1,2,3 \tag{9}$$

or as Neumann type

$$B[u_i] = n_j \frac{\partial}{\partial x_j}[u_i] = f_i(x) \qquad i = 1,2,3. \tag{10}$$

where n_j represents the unit outward surface normal at x.

In the case of adiabatic boundary conditions, the value of the boundary operator, $f_i(x)$ will be zero, representing no flux of "heat" across the boundary. In the case of Dirichlet boundaries, the value of $f_i(x)$ will represent the enforced displacement at that location.

With this definition, the Hermitian RBF formula for each component of displacement, u_i, may be written as:

$$u_i(x) = \sum_{1}^{N1} \alpha_{i,j} \psi\left(\left\|x - \xi_j\right\|\right) + \sum_{N1+1}^{N1+N2} \alpha_{i,j} B\left[\psi\left(\left\|x - \xi_j\right\|\right)\right] + \sum_{N1+N2+1}^{N1+N2+N3} \alpha_{i,j} L\left[\psi\left(\left\|x - \xi_j\right\|\right)\right] + \alpha_{i,N+1} \tag{11}$$

Where N1 represents the number of solution centres, N2 represents the number of boundary centres, and N3 represents the number of PDE centres within the collocation stencil. Since we consider the multiquadric RBF function with $(m = 1)$, the polynomial constrain reduces to the addition of a constant term.

This formula represents three independent reconstructions for the three components of displacement, which we model as obeying the heat equation. By determining the values of α_{ij}, the reconstruction formula may be used to obtain the displacement at any location within the domain of the RBF collocation.

To obtain the collocation matrix we reconstruct the value of u_i at solution centres, reconstruct $B[u_i]$ at boundary centres, and reconstruct $L[u_i]$ at PDE centres, using equation (11). This leads to the following system of equations:

$$\begin{bmatrix} \psi & B_\xi[\psi] & L_\xi[\psi] & 1 \\ B_x[\psi] & B_xB_\xi[\psi] & B_xL_\xi[\psi] & B_x[1] \\ L_x[\psi] & L_xB_\xi[\psi] & L_xL_\xi[\psi] & 0 \\ 1 & B_\xi[1] & 0 & 0 \end{bmatrix} \alpha_i = \begin{bmatrix} u_i \\ f_i \\ 0 \\ 0 \end{bmatrix} \qquad i = 1,2,3 \qquad (12)$$

In the above matrix equation, the operators with subscript ξ are applied to the trial points (i.e. functional centres), and the operators with subscript x are applied to the test points (i.e. locations at which (11) is enforced to generate the matrix system (12)). This linear system is symmetric, and was shown by Wu (1998) to be non-singular so long as no two collocation points sharing a linearly dependent operator are placed at the same location.

In our approach, we form an Hermitian collocation system of the form (12) for each of the N local stencils, i.e.

$$A^{(k)}\alpha_i^{(k)} = d_i^{(k)} \qquad k = 1,...,N \qquad (13)$$

Here $A^{(k)}$ represents the collocation matrix for collocation system k, $d_i^{(k)}$ represents the data-vector for the i^{th} displacement component in system k, and $\alpha_i^{(k)}$ represents the corresponding system weights. Note that, at the solution centres, represented by the first row-block of the matrix system as set out in equation (12), the value of the displacements u_{ij} is presently unknown, and will be determined only after solution of the following sparse global assembly.

To obtain the sparse global matrix, we reconstruct the three solution components, as defined by equation (11), at the system centrepoint $x_c^{(k)}$ (i.e. at the mesh-node around which local system k has been formed). Writing this reconstruction in vector form we have

$$u_i^{(k)}\left(x_c^{(k)}\right) = H^{(k)}\left(x_c^{(k)}\right)\alpha_i^{(k)} \qquad (14)$$

Where $H^{(k)}\left(x_c^{(k)}\right)$ is identified as a reconstruction vector for system k at its centrepoint $x_c^{(k)}$. By rearranging this formula, we can obtain the value of u_i at $x_c^{(k)}$ in terms of the data-vector $d_i^{(k)}$:

$$\begin{aligned} u_i^{(k)}\left(x_c^{(k)}\right) &= H^{(k)}\left(x_c^{(k)}\right)\alpha_i^{(k)} \\ &= H^{(k)}\left(x_c^{(k)}\right)\left[A^{(k)}\right]^{-1} d_i^{(k)} \\ &= W^{(k)}\left(x_c^{(k)}\right) d_i^{(k)} \end{aligned} \qquad (15)$$

Here $W^{(k)}\left(x_c^{(k)}\right) = H^{(k)}\left(x_c^{(k)}\right)\left[A^{(k)}\right]^{-1}$ is a stencil weights vector, which expresses the value of the solution field u_i at the system centrepoint, in terms of the entries in the data vector $d_i^{(k)}$. The data vector $d_i^{(k)}$ contains the unknown displacement values at surrounding nodes, therefore, by performing the reconstruction at every solution centre within the domain, a series of N simultaneous equations are formed for the N unknown values of u_i at the system centrepoints. The solution of this sparse linear system therefore provides the displacement at each of the N internal mesh nodes.

Once the values of the displacements u_i are obtained at the internal mesh nodes, and these values have been fed back into the local system data vectors $d_i^{(k)}$, the displacement value at any location within the solution domain may be obtained by forming a solution weights vector $W^{(k)}(x)$ for any x within the support domain of system k, and multiplying with the associated data-vector $d_i^{(k)}$. In this way, the displacement at the surface nodes may be obtained by reconstructing from any number of RBF systems which include it in their stencil.

4: Relaxation procedure and surface / edge constraint

The relaxation procedure is driven by the movement of the crack-front through the domain, as determined by the crack growth integration process from the previous FE iteration. The nodes of the elements immediately surrounding the crack-front, referred to as crack-block nodes (see section 5), have a non-zero displacement applied, allowing the “crack-block elements” to move with the motion of the crack-front. The relaxation procedure therefore aims to translate these enforced displacements smoothly throughout the domain, in order to retain a high-quality mesh.

Since the crack-front can be expected to intersect the domain boundaries at one or more locations, it is essential that nodes on the surfaces and edges of the domain are allowed to move. In order to allow the nodes on the domain surfaces and edges to be properly constrained to their respective geometries, the relaxation procedure follows a three-stage process: The first stage predicts the motion of edge nodes and fixes their position onto the domain edges, the second stage predicts the motion of surface nodes and defines their motion over their respective surfaces, and the final stage predicts the resulting motion of all nodes internal to the domain.

In the first stage of the procedure only the domain corners are fixed, with adiabatic boundary conditions applied over all remaining edge and surface nodes. The RBF finite collocation procedure is then followed, as described in Section 3, allowing the predicted displacement to be computed at each edge

node within the domain. The deformation field resulting from the RBF procedure will inevitably predict some out-of-edge displacement for edge nodes, which must be mapped back onto the edge at an appropriate location.

By dividing each geometric edge into line-segments, based on data from the original uncracked mesh, it is possible to identify a unique location on the edge which is closest to the displaced edge node position. The edge node is then mapped to this position, becoming a fixed displacement constraint for the next iteration. In this way, the predicted motion in the direction of the edge is respected, while constraining the motion to the correct geometry; edge nodes are allowed to "slide" along their respective edges, but are not permitted to leave the edge.

At the second stage of the procedure, the edge nodes have already been assigned a displacement, and therefore become fixed-displacement Dirichlet boundary conditions, together with the assigned displacement at the crack-block nodes (which remains unchanged from the previous stage). The remaining non-edge surface nodes are again assigned an adiabatic boundary condition, which allows their motion to be predicted by the RBF relaxation procedure.

In order to properly constrain the motion of surface nodes in the case of complex geometric surfaces, each surface is tessellated with a number of triangular facets. In the case of hexahedral elements, as utilised by the Zencrack software (see Section 5), four triangular facets are created for each quadrilateral element face which lies on the domain surface, using the centre of the face as a guide. The displacement at the surface nodes, as predicted by this second RBF deformation, will typically contain some out-of-surface component. To compensate for this, the surface nodes are projected along a line, as defined by their surface-normal at the previous iteration. The triangular facets which are close to the node are then examined for interception with this projection line. Because the surface has been discretised by a finite number of triangular planes, the interception location is unique. The surface nodes are then constrained to this location on the surface ready for the next and final iteration. As was the case with the edge nodes, this procedure allows surface nodes to slide along their respective surfaces in a natural fashion.

It is important to note that, for every crack front, a trailing crack surface is generated as the crack front moves through the domain. This crack surface is treated in precisely the same way as for the original geometric surfaces, being tessellated with surface facets. Nodes which must be constrained to the crack-surface are then mapped onto it in exactly the same fashion, and are therefore able to slide over the crack surface as needed.

The third and final stage of the relaxation procedure uses the displacement of surface and edge nodes as computed in the previous two stages, along with the

enforced displacements at the crack-block nodes, in order to predict the motion of internal nodes – thereby relaxing the entire mesh around the motion of the crack-front. At this stage there are no adiabatic boundary conditions, since all surface nodes have been assigned an applied displacement in previous stages.

The three-stage relaxation procedure allows the element quality to be maintained on approach to the domain edges and boundaries. In principle it is be possible to relax all nodes; surface edge and internal, based on the result of the first stage (i.e. by fixing only the corner and crack front nodes). However, in the case that out-of-plane deformations are predicted that are of a size approaching the element scale, elements immediately adjacent to surfaces or edges would become highly elongated or even inverted. Such an approach therefore would be suitable only for very small movements of the crack front. By adopting the three-stage procedure, i.e. by moving edge, surface and internal nodes separately, the relaxation is effective for much larger displacements of the crack-front, and therefore significantly more robust.

5: Zencrack: An FEA tool for 3D crack analysis on complex geometries

The proposed new RBF relaxation technique has been implemented in the Zencrack fracture mechanics package. Zencrack allows analysis of one-off crack positions and general 3D non-planar crack growth under fatigue and/or time dependent crack growth loading conditions. The Zencrack analysis procedure is summarised in Figure 3. The mesh relaxation technique occurs during the re-meshing stage as the crack front advances through the model.

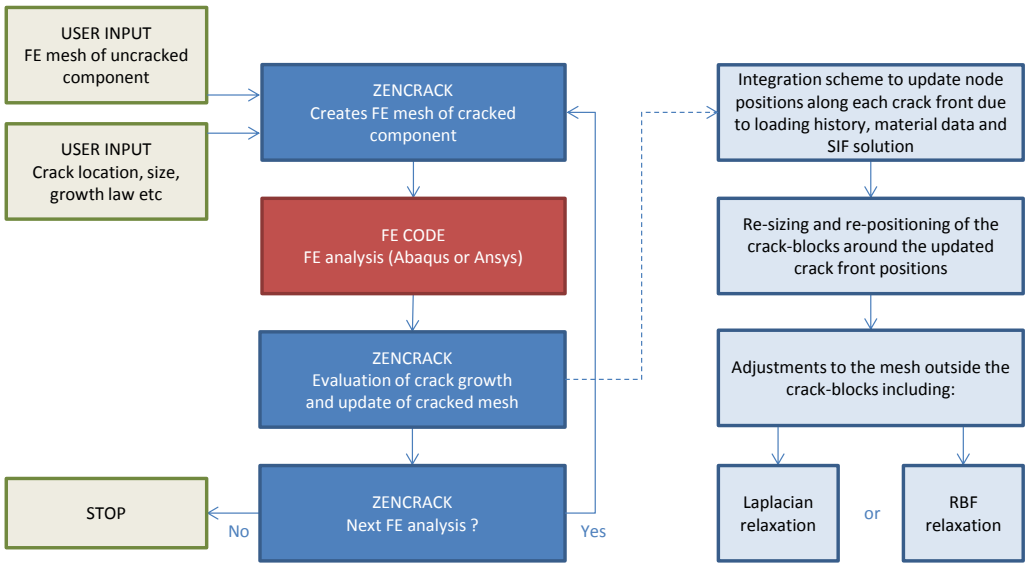

Figure 3: Flowchart summarising analysis procedure and use of mesh relaxation.

The re-meshing procedure in Zencrack adopts the use of "crack-blocks" to model the details at the crack front. One or more crack-blocks replace elements

of a user supplied uncracked mesh. The meshing process for each crack front advancement has three stages, as shown in Figure 3. First the new crack front position is identified. This is a consequence of the crack growth integration scheme operating on the results of f.e. analysis of the previous crack position in conjunction with a loading history and crack growth law. The updated crack position is described by a series of nodes in space. The crack-blocks are then oriented around the new crack front position. The nodes outside the crack-blocks are then moved to appropriate new positions to define the revised mesh outside the crack-blocks. This final calculation is where mesh relaxation takes place. An example of the procedure (using the original Laplacian method) is shown in Figure 4 to Figure 7.

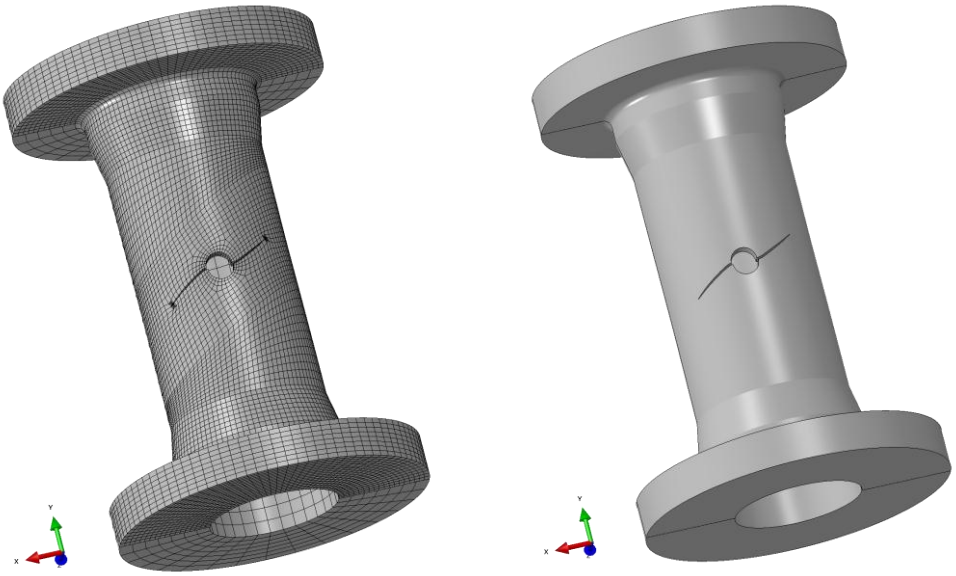

(a) (b)

Figure 4: Deformed plots showing crack positions after growth of starter cracks at the hole (a) with mesh shown (b) with mesh removed to show the crack paths more clearly

Figure 4 shows the final crack positions for two cracks growing from a hole in a circular shaft test specimen under cyclic tension and torsion loading. In Figure 5(a) the uncracked mesh is shown with the target elements for replacement by crack-blocks highlighted in yellow. Figure 5(b) shows the initial cracked mesh with the crack-blocks in place. Figure 5(c) and 5(d) show two advanced crack positions during the analysis. Clearly, the elements surrounding the crack-blocks in each mesh have different distributions as the mesh has moved to accommodate the crack growth. This movement is the result of the mesh relaxation process. Figure 6 shows a cut-away at analysis step 26 with crack profiles superimposed. This demonstrates how the crack-blocks have been oriented around the current crack position with mesh relaxation having been applied to the surrounding nodes. Once the crack-block

orientations are calculated, the nodes of the crack-blocks become “fixed nodes” in terms of the mesh relaxation process which follows i.e. they are not moved during mesh relaxation.

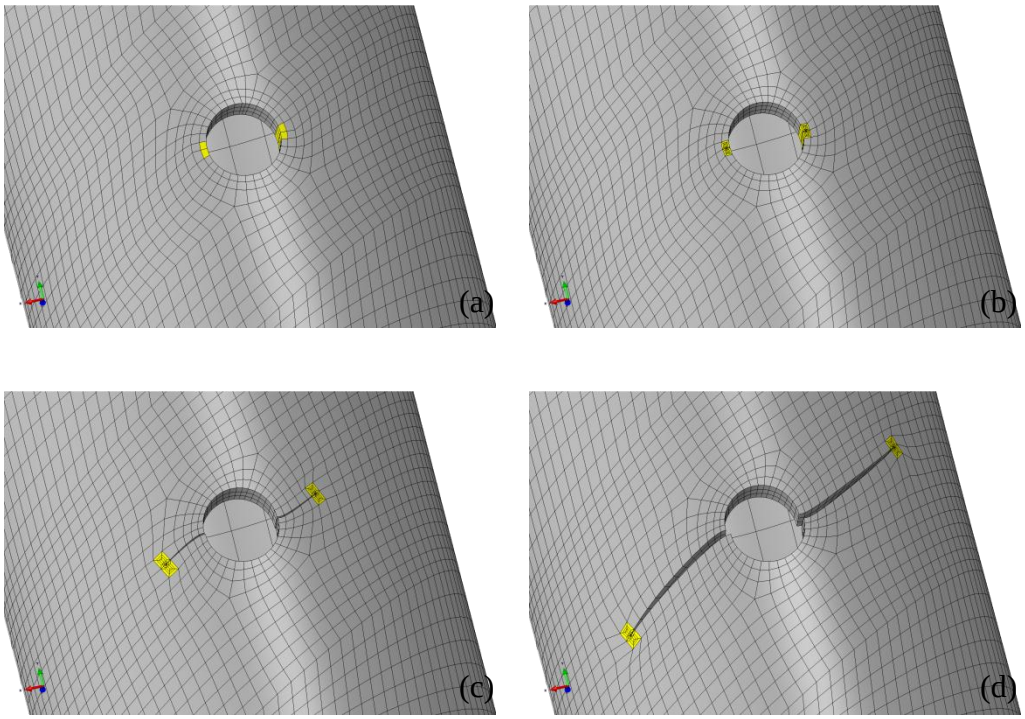

Figure 5: Stages of the growth analysis with the crack-block region highlighted in yellow (a) uncracked mesh (b) initial cracked mesh (c) cracked mesh at step 26 (d) cracked mesh at step 46

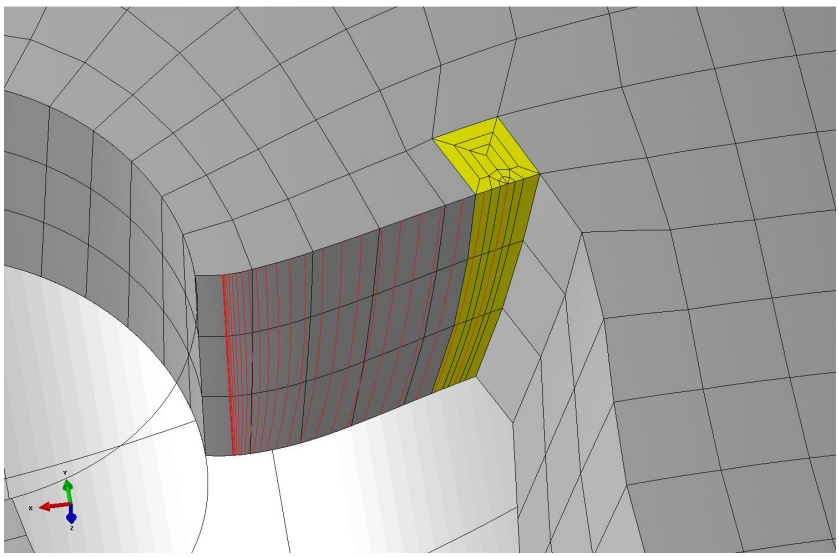

Figure 6: Cut-away at step 26 showing the way the crack-blocks are oriented around the current crack front with crack face nodes fitted to the crack path

6: Examples of crack propagation using RBF relaxation

Figure 7 shows the propagation of a simple, linearly-advancing crack front. The mesh includes biasing of elements to further compare the RBF and Laplacian procedures. The mesh resulting from RBF relaxation is shown in Figure 7(a), and that resulting from Laplacian relaxation is shown in Figure 7(b). In this case there is little relaxation of the mesh required around the crack-front; however, the RBF relaxation better retains the user-defined element biasing that is present in the initial mesh. By contrast, the Laplacian method attempts to normalise elements that are further from the crack-front. By computing a global displacement field, rather than adjusting individual elements, mesh features present in the original uncracked mesh are better retained during the crack advancement procedure.

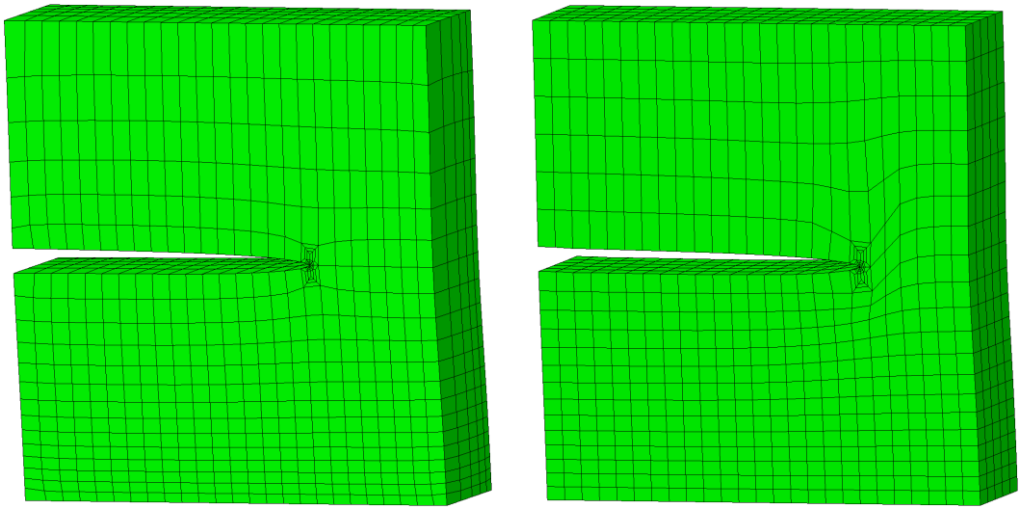

(a) RBF relaxation **(b) Laplace relaxation**

Figure 7: Advancement of a simple linear crack with Laplacian and RBF relaxation (exaggerated deformation scale).

The advancement of a crack generated within a plate with a hole is shown in Figure 8. The crack starts next to a curved surface, requiring careful constraint of nodes on the curved surface and edges. As the crack front advances into the domain, the mesh is relaxed around the crack-block elements. Elements that lie adjacent to the trailing crack surface are fitted to their respective sides of the crack.

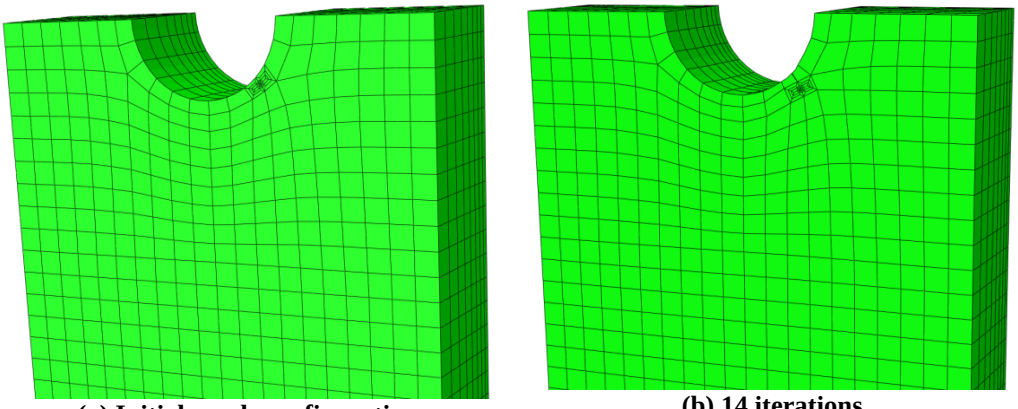

(a) Initial crack-configuration **(b) 14 iterations**

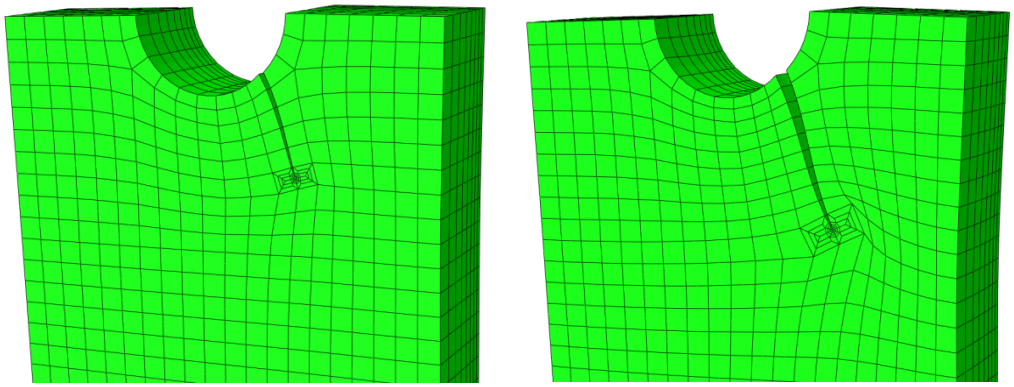

(c) 27 iterations **(d) 36 iterations**

Figure 8: Advancement of a crack through a plate with a circular hole.

The relatively coarse mesh in this example acts as a "stress test" for the relaxation algorithm. Here the RBF method can be seen to improve on the Laplace relaxation approach. Figure 9 shows the 36th iteration of the Zencrack crack-advancement process, using RBF and Laplace mesh relaxation respectively. Using the Laplace approach it is necessary to significantly reduce the size of the crack-blocks in order to avoid inverting the elements surrounding the crack-front, which is unnecessary with the RBF relaxation at this stage in the simulation. In addition, the Laplace method once again removes the mesh-grading that is present in the z-direction within the original mesh; elements close to the crack-front have the grading properly enforced, but elements further away become almost uniform. In the RBF relaxation the grading is properly maintained.

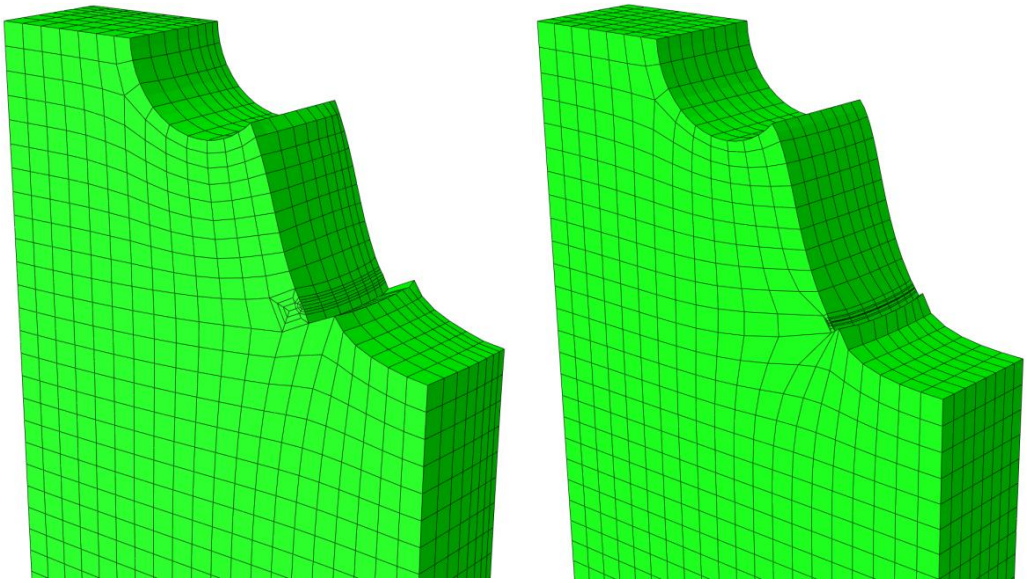

(a) RBF relaxation **(b) Laplace relaxation**

Figure 9: Plate with a circular hole: Cutaway showing element quality over the crack-surface, at 36 iterations.

The relaxation may be applied to complex, curved geometries that include multiple fractures. Figure 10 shows the RBF relaxation algorithm at work during the simulation of two fractures propagating through a square section with a swept, circular cut. To account for the large difference in the size of the elements at either end of the two crack-fronts, the crack-block elements at the lower surface expand as the crack-front advances, with the surrounding elements relaxed around them.

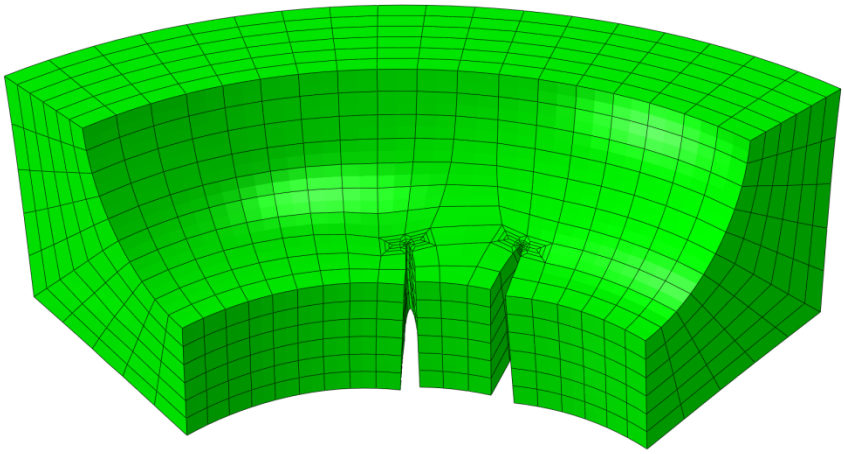

(a) Top-view

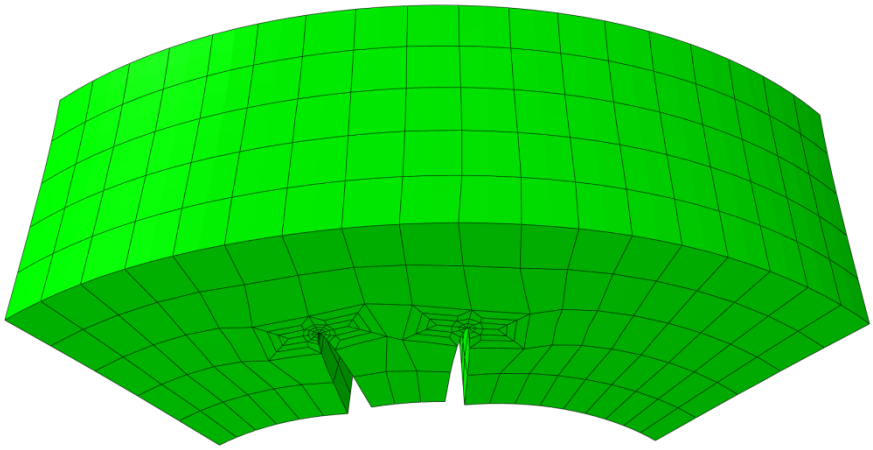

(b) bottom view

Figure 10: Two cracks growing through a domain with curved cut-out.

7: Conclusions

A novel procedure has been described to allow the relaxation of a finite element mesh during the simulation of crack propagation in complex 3D models. The proposed method is based on the solution of the steady heat equation across the entire solution domain, using a numerical technique based on overlapping local radial basis function collocation systems. Unlike other full-domain RBF collocation approaches, the computational cost of the proposed method scales linearly with problem size, making it suitable for application to large models.

The method is successfully able to relax the finite element mesh around the moving crack-front. By defining a smooth deformation field propagating from the crack tip, a good element quality may be maintained throughout the mesh. Compared to the Laplace relaxation method, user-defined features in the original mesh such as grading of aspect-ratio are better maintained using the RBF relaxation.

REFERENCES

Bos, F., Numerical simulations of flapping foil and wing aerodynamics: Mesh deformation using radial basis functions, PhD thesis, Technische Universiteit Delft, 2010

Divo, E. & Kassab, A., An efficient localised radial basis function meshless method for fluid flow and conjugate heat transfer, Journal of Heat Transfer, 2007, 129, 124-136

Fasshauer, G. E., M'ehaut'e, A. L.; Rabut, C. & Schumaker, L. (Eds.)
Solving partial differential equations by collocation with radial basis functions, Surface Fitting and Multiresolution Methods, Vanderbilt University Press, 1997, 131-138

Fornberg, B. & Zuev, J., The Runge phenomenon and spatially variable shape parameters in RBF interpolation, Comput. Math. Appl., 2007, 54, 379-398

Franke, R., Scattered data interpolation: Tests of some methods, Math. Comp., 1982, 38, 181-200

Hardy, R., Multiquadric equations of topography and other irregular surfaces J. Geophys. Res., 1971, 176, 1905-1915

Jones, R.E., QMESH: A Self-Organizing Mesh Generation Program, Sandia Report SLA-73-1088, Sandia National Laboratories, p.23, (1974).

Kansa, E. & Carlson, R., Improved accuracy of multiquadric interpolation using variable shape parameters, Comput. Math. Appl., 1992, 24, 99-120

Schaback, R., Jetter, K.; Schumaker, L. & Uteras, F. (Eds.), Comparison of radial basis function interpolants, Multivariate Approximation: From CAGD to Wavelets., World Scientific, Singapore, 1993, 293-305

Stevens, D.; Power, H.; Lees, M. & Morvan, H., The use of PDE centres in the local RBF Hermitian method for 3D Convective-Diffusion problems, J. Comput. Phys., 2009, 228, 4606-4624

Wendland, H., Piecewise polynomial, positive definite and compactly supported radial basis functions of minimal degree, Adv. Comput. Math., 1995, 4, 389-396

Wright, G. & Fornberg, B., Scattered node compact finite difference-type formulas generated from radial basis functions, J. of Comput. Phys., 2006, 212, 99-123

Wu, Z., Compactly supported positive definite radial basis functions
Adv. Comput. Math., 1995, 4, 75-97

Wu, Z., Chen, Z.; Y.Li; Micchelli, C.; Xu, Y. & Dekkon, M. (Eds.)
Solving PDEs with radial basis functions and the error estimation
Adv. in Comput. Math., Lectures in Pure and Applied Mathematics, 1998, 202

Zencrack software, Zentech International Limited, www.zentech.co.uk